IEEE Access
Multidisciplinary | Rapid Review | Open Access Journal

Received October 15, 2018, accepted October 31, 2018, date of publication November 21, 2018,
date of current version December 19, 2018.

Digital Object Identifier 10.1109/ACCESS.2018.2881430

Selection and Fusion of Spectral Indices to Improve Water Body Discrimination

GABRIELA CALVARIO SÁNCHEZ[1], OSCAR DALMAU[2], TERESA E. ALARCÓN[3], BASILIO SIERRA[1], AND CARMEN HERNÁNDEZ[1,4]

[1]Departamento de Ciencias de la Computación e Inteligencia Artificial, Universidad del País Vasco UPV/EHU, 20018 Donostia-San Sebastián, Spain
[2]Centro de Investigación en Matemáticas, Guanajuato 36240, México
[3]Departamento de Ciencias Computacionales e Ingeniería, Centro Universitario de los Valles, Ameca 46600, México
[4]Centro de Investigação e Tecnologias Agro-ambientais e Biológicas, Universidade de Trás-os-Montes e Alto Douro, 5001-801 Vila Real, Portugal

Corresponding author: Teresa E. Alarcón (teresa.alarcon@profesores.valles.udg.mx)

This work was supported in part by the Consejo Nacional de Ciencia y Tecnologia (CONACYT), Mexico, under Grant 258033, in part by the Basque Government under Grant IT900-16, and in part by the Spanish Ministry of Economy and Competitiveness (MINECO/FEDER) under Grant TIN2015-64395-R. The work of G. C. Sánchez was supported by CONACYT through a scholarship for her Ph.D. studies.

ABSTRACT Spectral indices are widely used to emphasize water body information in satellite images. The selection of the appropriate index is one of the tasks that the remote sensing community faces when water bodies are studied. In this paper, we propose an approach for the selecting and fusing of spectral indices, in order to improve water discrimination. First, we compute several spectral indices and analyze their discrimination power, taking into account the accuracy value. Through a hierarchical clustering applied only on indices with accuracy value greater than a certain threshold, we cluster the water indices into different groups. The result of the clustering depends on two factors: the discrimination capacity of the computed indices and the features of the studied water body. Indices in each group are fused by means of a linear combination. Therefore, we obtain an adaptive fusion of different spectral indices. The previous information is used to compute the likelihoods belonging to water and non-water. These values are the inputs for a probabilistic classification framework named Gaussian–Markov measure field. According to our experimental work, the proposed selection and fusion approach improves the discrimination power of the studied indices.

INDEX TERMS Water resources, spectral water index, remote sensing, spectral analysis, optimization.

I. INTRODUCTION

Water bodies are very important resources for maintaining equilibrium in the ecosystem, as well as social and economic development of a region or country. Therefore, the study of them is essential for establishing policies for the use and protection of water resources.

New technologies, particularly the employment of remote sensing and digital processing of satellite images, have provided synoptic and large scale observations, which has favored the investigation of water resources. Several techniques are used to study water bodies. Unsupervised and supervised methods, and the combination of both are general strategies used for water body extraction [1]. In the unsupervised algorithms, the grouping process is based on the feature space analysis of the image without information about classes. Examples of unsupervised algorithms are k-means [2], [3] and Iterative Self-Organizing Data Analysis Technique (ISODATA) [4]. Similar to k-means, ISODATA is focused on the central tendencies and major structures of the data. Both methods are iterative algorithms, but unlike k-means, ISODATA includes a refinement step based on the splitting and merging of clusters. On the other hand, the supervised techniques require a training dataset with data consisting on a feature vector and the corresponding category or class. In the case of water segmentation, the algorithms need samples of pixels labelled as water/non-water (ground truth), that typically are given by an expert. Examples of supervised algorithms used for water classification are the random forest algorithm [5] and the J48 decision tree [6]. Moreover, the Support vector machine (SVM) [7] and artificial neural networks [8] are used in remote sensing for water recognition.

Spectral water indices, WI, are frequently used as descriptors for all aforementioned approaches. Among of them are: Normalized difference water index, NDWI [9], and modification of it such as NDWI1, NDWI5 in [10] and modified

normalized water index in [11]; water ratio index, WRI, in [12] and [13] and automatic water index for shadow, $AWEI_{sh}$, and no shadow conditions, $AWEI_{nsh}$ in [14]. The normalized difference moisture index, NDMI [15] and normalized difference vegetation index, NDVI [16] are indices frequently used to study vegetation, but due to their capacity to track the water stress in land coverage [17], both indices are useful to analyze water bodies. In [18], the perceptron model leads to accurate discrimination of water bodies. The considered descriptors were the MNDWI [11] and the reflectance in different spectral bands, obtained from Landsat TM imagery. The proposal in [19] allowed the analysis of the spatio-temporal changes in a water body using images from Landsat TM and ETM+ images. The experimental work took into account SVM [7] and three spectral indices: NDWI [9], MNDWI [11], AWEI [14]. The SVM and NDWI were superior to other strategies. Research done in [20] combines a pixel-based approach such as NDWI and object oriented model [21], [22] on Sentinel-2 satellite images. This combination is justified by the fact that it is hard to discriminate objects with similar spectral response using only spectral indices, especially when this pixel-based approach tries to separate water bodies from another object with a low albedo, for instance: shadows, built-up areas, snow and ice [20]. Several indices have been proposed to avoid the mentioned problem [11], [14]. However there are still problems to finding the index or combination of appropriate indices that leads to an optimal descriptor that would facilitate the analysis of each water body. The results obtained by different spectral indices used for water detection, are not always reliable. Furthermore, the threshold values computed to discriminate water and non-water change with the contextual information and location of the water body [14]. Additionally, the spectral range of the bands varies from one sensor to another. Therefore the results obtained through spectral indices depend also on the sensor resolution.

In this work, we include several spectral indices and analyze the discrimination capacity of each of them. Firstly, indices with an accuracy value higher than a certain threshold are selected. Then, through a hierarchical clustering applied on selected indices, we obtain three groups. Indices in each group are mixed by means of a linear combination, leading to new three indices. Coefficients in the combination are calculated in three different ways: average and correlation sign, fisher discrimination analysis and best index in the group. The information given by the combination, together with the segmentation given by an expert are used to compute the likelihood values for a probabilistic segmentation framework, in particular, in this work a robust version of the Gaussian Markov Measure Field models is applied [23], [24].

The studied images correspond to Chapala lake, the Infiernillo and Nezahualcoyotl reservoirs in Mexico and they are Landsat 8 OLI images acquired through a USGS Global Visualization Viewer site http://glovis.usgs.gov.

The structure of this paper is the following: in Section 2 we briefly review the spectral indices included in the research, in Section 3 we explain the proposal. Section 4 describes the studied areas. Section 5 and 6 are dedicated to the experimental setup and discussion of the results respectively. In Section 7 the conclusions are given.

II. STUDIED WATER INDICES

Table 1 contains all the indices considered in the proposal, including the formulae and the spectral range of the bands used to compute the index in the referenced papers (columns 2, 3 and 4).

In Table 1, ρ represents top-of-atmosphere-reflectances calculated according to [27].

The coefficients, for $AWEI_{nsh}$ and $AWEI_{sh}$ in the linear combinations were provided in [14]. Feyisa *et al.* [14] calculated these coefficients through an iterative procedure that maximizes the separability between water and non-water; they are used for the study of any water body and the facts related to the acquisition and the structure of the object are no longer considered when the index is applied.

The capability of detecting water bodies, for all included indices, depends on the resolution of the sensors and on the structure of water body being studied.

III. THE PROPOSAL

In general, the aforementioned spectral indices have proven to present a high discrimination power for water body detection. However, in some situations the discrimination power may decrease due to the particular conditions of the water body, cloudy weather, loss of information during the acquisition process and misleading data because of difficulty in discriminating water from other objects on the Earth's surface with low albedo. On the other hand, it has been observed that when applying the typical threshold for each water index these methods do not always yield good results [9], [11]. For the previous reason, some research has been carried out in order to find a good threshold, however these thresholds have been unstable, see [14] for details.

In this paper, we present a strategy based on the selection and fusion of spectral indices, taking into account the discriminant power of each studied index. The idea is to combine indices to form new adaptive indices (or layers) that can be used as the input of a classification method. In this work, for the classification step, we use a probabilistic segmentation method based on a robust version of the Gaussian Markov Measure Field models [23], [24].

Firstly, from indices presented in Table 1, we select the most relevant indices in order to reduce their number while maintaining, as much as possible, the discriminatory power. Secondly, we cluster the selected indices in K groups and finally, we compute new adaptive indices as follows:

$$L_i = \sum_{j=1}^{N_i} \alpha_i^j I_{ij}; \quad i = 1, 2, \cdots, K; \tag{1}$$

where N_i is the number of spectral indices in the i-th cluster, I_{ij} represents an spectral index j in group i, α_i^j are the weights

TABLE 1. Included indices in the research. ρ represents the reflectances values. The spectral band ranges, in the third column, correspond to the resolution of the sensors in the references provided in the fourth column.

Name	Formulae	Satellite Band wavelength (μm)	Reference
NDWI	$\frac{\rho_2 - \rho_4}{\rho_2 + \rho_4}$ $\frac{Green - NIR}{Green + NIR}$	Landsat 5 TM Green band → 0.52-0.60 NIR band → 0.76-0.90	[9]
NDWI1	$\frac{\rho_7 - \rho_5}{\rho_7 + \rho_5}$ $\frac{SWIR2 - SWIR1}{SWIR2 + SWIR1}$	Landsat TM/ETM+ SWIR2 band → 2.06-2.34 SWIR1 band → 1.55-1.75	[10]
NDWI5	$\frac{\rho_7 - \rho_2}{\rho_7 + \rho_2}$ $\frac{SWIR2 - Green}{SWIR2 + Green}$	Landsat TM/ETM+ SWIR2 band → 2.06-2.34 Green band → 0.52-0.60	[10]
MNDWI	$\frac{\rho_2 - \rho_5}{\rho_2 + \rho_5}$ $\frac{Green - SWIR}{Green + SWIR}$	Landsat TM/ETM+ Green band → 0.52-0.60 SWIR1 band → 1.55-1.75	[11]
NDPI	$\frac{\rho_1 - \rho_4}{\rho_1 + \rho_4}$ $\frac{Green - MIR}{Green + MIR}$	SPOT5 Green band → 0.50-0.59 MIR band → 1.58-1.75	[25]
NDSI	$\frac{\rho_2 - \rho_5}{\rho_2 + \rho_5}$ $\frac{Green - SWIR}{Green + SWIR}$	Landsat 5 TM Green band → 0.52-0.60 SWIR1 band → 1.55-1.75	[26]
NDVI	$\frac{\rho_6 - \rho_5}{\rho_6 + \rho_6}$ $\frac{NIR - Red}{NIR + Red}$	Landsat 1 (ERTS 1) NIR band → 0.7-0.8 Red band → 0.6-0.7	[16]
WRI	$\frac{\rho_2 + \rho_3}{\rho_4 + \rho_5}$ $\frac{Green + Red}{NIR + SWIR}$	Landsat ETM+ Green band → 0.52-0.60 Red band → 0.63-0.69 NIR band → 0.77-0.90 SWIR1 band → 1.55-1.75	[12], [13]
$AWEI_{sh}$ $AWEI_{nsh}$	$\rho_1 + 2.5\rho_2 - 1.5(\rho_4 + \rho_5) - 0.25\rho_7$ $Blue + 2.5Green - 1.5(NIR + MIR1) - 0.25MIR2$ $4(\rho_2 - \rho_5) - (0.25\rho_4 + 2.75\rho_7)$ $4(Green - MIR1) - (0.25MIR + 2.75MIR2)$	Landsat 5 TM+ Blue band → 0.45-0.52 Green band → 0.52-0.60 Red band → 0.63-0.69 NIR band → 0.76-0.90 MIR1 band → 1.55-1.75 MIR2 band → 2.08-2.35	[14]

of the linear combination and K is the number of clusters. Therefore, the new adaptive index L_i is basically a linear combination of different spectral indices.

The general idea of the proposed method is to reduce the dimensionality while keeping the separability between classes. In order to select the most relevant indices, we

threshold the corresponding image, by means of Otsu [28]. This is a dynamic threshold method which is widely used in image processing. It consists of maximizing the variance between classes and minimizing the intraclass variance. This allows us to obtain an optimal threshold value for the separation between water and non water bodies. Then, we compute the discrimination capacity of each water index through the accuracy measure. Indices with an accuracy value higher than a certain threshold are selected. The training samples for computing accuracy values are randomly taken from the ground truth, i.e. water/non water regions manually labelled, provided by an expert.

The described step may reduce the feature space, but more importantly, it allows us to preserve the water indices with high discriminatory power. In the second step, after selecting the water indices with higher accuracy, we propose to cluster the selected indices in three different groups or clusters. In this work we use a hierarchical clustering algorithm [29]. Finally, for computing the new adaptive indices in (1) we propose three strategies. We can use the average with sign for each cluster, i.e., $\alpha_i^j = \frac{s_j}{N_i}$, for $j = 1, 2, \cdots, N_i$, where s_j is the sign of the correlation between the index with best classification performance in the cluster i-th and the index I_j of the same cluster. Another proposed method is to highlight the contrast between the classes by maximizing the Fisher's criterion:

$$\mathrm{FDR}(\boldsymbol{\alpha}) = \frac{\boldsymbol{\alpha}^T \boldsymbol{S}_b \boldsymbol{\alpha}}{\boldsymbol{\alpha}^T \boldsymbol{S}_w \boldsymbol{\alpha}}, \tag{2}$$

where $\boldsymbol{S}_b$ is the between-class scatter matrix and $\boldsymbol{S}_w$ the within-class scatter matrix [30]. The solution is computed directly by:

$$\boldsymbol{\alpha} = \boldsymbol{S}_w^{-1}(\boldsymbol{m}_1 - \boldsymbol{m}_2), \tag{3}$$

where $\boldsymbol{m}_1$, $\boldsymbol{m}_2$ are the mean of the two classes, respectively [30]. The third proposed alternative simply assigns 1 to the coefficient corresponding to the spectral index with the best classification performance, and 0 to the remainder, i.e., selects the best spectral index for each cluster.

Here, we have proposed three different ways of obtaining the coefficients in (1). In practice, the selection of the weights of the linear combination depends on the analyzed image and the particular conditions of the water body. Regardless of the strategy used to calculate the coefficients of the linear combination, we obtain an adaptive fusion of different spectral indices. The new adaptive indices depend on the particular analyzed image, i.e., we cannot specify the spectral index to be selected nor the cluster to which it will belong.

In summary, we apply the previous fusion method to a sample of water pixels and non-water pixels. The sample is simply obtained from the ground truth provided by an expert. Then, we use the result of the linear combination to train a classification algorithm and finally we apply the classifier to the whole image.

Although, the fusion of the spectral indices can be used as a training set of any classification algorithm, for example: a neural network or SVM; here we use a probabilistic segmentation method because this type of method takes into account the local information of the image, which allows producing less granular segmentations. Additionally, this method has recently been used successfully in satellite images for crop classification [23], [24]. For the sake of completeness we provide some details of a robust variant of the GMMF used in this work. The GMMF solves the problem of determining the probability $p_k(r)$ of each pixel or site r of the image to belong to class k. The GMMF is formulated as the following optimization problem:

$$\begin{aligned} \boldsymbol{p}^* = \arg\min_{\boldsymbol{p}} & \sum_{r\in\mathcal{L}} \sum_{k\in\mathcal{K}} (p_k(r) - v_k(r))^2 \\ & + \lambda \sum_{s\in\mathcal{N}_r} \omega_{rs}(p_k(r) - p_k(s))^2, \end{aligned} \tag{4}$$

where $\mathcal{L}$ is the set of pixels in the region of interest, $\lambda > 0$ is a regularization parameter, $\mathcal{N}_r$ is the set of neighboring pixels to site r, $\mathcal{K} = \{0, 1\}$ is the set of classes, $v_k(r)$ represents the likelihood of pixel r to belong to class k. The likelihoods $v_k(r)$ are computed from the layers L_i and histograms obtained from expert information, see details in [24]. The weight function $\omega_{rs} \in [0, 1]$ allows control of the edges between classes. Here we use:

$$\omega_{rs} = \frac{\mu}{\mu + \|v(r) - v(s)\|_2^2}, \tag{5}$$

such that $\omega_{rs} \approx 1$ if the sites r, s most likely belong to the same class and $\omega_{rs} \approx 0$ otherwise.

Finally, the solution of the optimization problem (4) yields the following Gauss-Seidel scheme:

$$p_k(r) = \frac{v_k(r) + \lambda \sum_{s\in\mathcal{N}_r} \omega_{rs} p_k(s)}{1 + \lambda \sum_{s\in\mathcal{N}_r} \omega_{rs}}, \tag{6}$$

This is an iterative algorithm in which the previous formula is repeated until convergence for each site r and each class k. Note however, that in our case, one just needs to apply the algorithm for one class, for example $k = 1$ and the other, $p_0(r)$ is simply computed as follows $p_0(r) = 1 - p_1(r)$. Figure 1 depicts the flowchart of the proposed algorithm.

IV. STUDY AREA

Three water bodies are included in this research: Chapala lake, the Infiernillo and Nezahualcoyotl reservoirs. The images were acquired from Landsat 8 satellite through a USGS Global Visualization Viewer site http://glovis.usgs.gov. The images have spatial resolution of 30 meters. The cloudiness level is very low, less than 10%, and does not affect the images corresponding to the analyzed water bodies. Table 2 summarizes some specifications of the study areas.

Chapala lake is located in Mexico and it is the largest natural lake in the country. Chapala is located in the eastern part of the state of Jalisco and in the northwestern part of Michoacan state in western Mexico, within latitude N20°15′00″ and

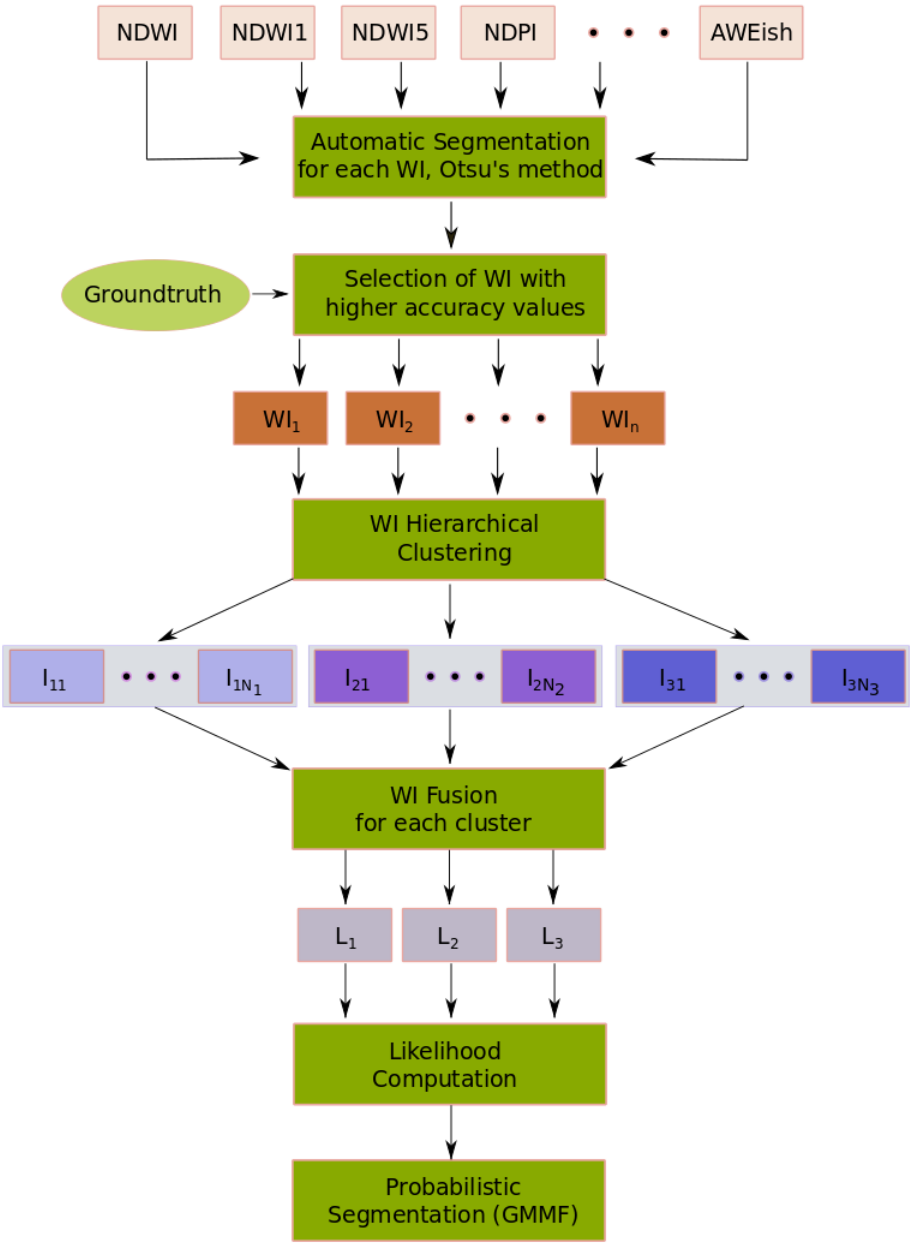

FIGURE 1. Flowchart of the proposed algorithm.

TABLE 2. Study areas.

Study Area	Path/Row	Acquisition Date	Water Body Type	Size
Chapala	29/46	2015-02-08	Lake	7731 x 7561
Infiernillo	28/47	2015-01-16	Reservoir	7711 x 7531
Nezahualcoyotl	22/48	2014-04-25	Reservoir	7781 x 7611

longitude W103°0′0″. Its approximate dimensions are 80 km from east to west and about 12.5 km from north to south. The Chapala lake is highly polluted with heavy metals and other toxic substances derived from industrial and agricultural wastes [31].

Infiernillo reservoir, is an embankment dam located between the states of Michoacan and Guerrero in Mexico with coordinates: latitude N18°16′23″ and longitude W101°53′34″. The dam supports a hydroelectric power station and it has 149 m of depth and 344 m of length.

FIGURE 2. Study water bodies. From left to right: Chapala lake, Infiernillo and Nezahualcoyotl reservoirs.

The total capacity of the dam is 12 500 000 000 m^3, http://www.conagua.gob.mx/atlas/.

The Nezahualcoyotl dam is located in Chiapas, Mexico. The coordinates of the reservoir are N17°10′43″ and W93°35′54″. This reservoir supports an hydroelectric power station. The depth and the length of the dam are 37.5 m and 480 m, respectively. The total capacity of the reservoir is about 10 596 000 000 m^3, http://www.conagua.gob.mx/atlas/.

Figure 2 shows the images of Chapala lake, Infiernillo and Nezahualcoyotl reservoirs. Chapala lake has a regular shape with a border that resembles an ellipse, Infiernillo and Nezahualcoyotl reservoirs have irregular shapes. These images also contain narrow rivers and small lakes that could be a challenge for some segmentation algorithms.

A. PREPROCESSING

The images were radiometrically calibrated and geometrically corrected. This correction was applied according to documentation in [32] and it was performed using Matlab (v.2012) [33], [34].

V. EXPERIMENTAL SETUP

For the experiment, we use the images described in Section IV. The results of our proposal is compared with the linear and the radial basis function Support Vector Machines. Additionally, we provided a comparison with all the spectral indices included in Section II. Here we present the results of the MNDWI, AWEInsh and NDVI spectral indices due to they obtained the best and most stable results.

In the case of the supervised methods, SVM and our proposal, we conducted experiments with different sizes of randomly selected training sets, from 1% to 50% of the number of pixels in the analyzed water body. The training sets were selected from the ground truth. In all cases, the performance of the algorithms was good and very stable. In the experiments that follow, the size of the training set is equal to the 1% of the number of pixels that belong to the water body in the corresponding image. For the SVM methods we use as feature vector the set of indices described in Table 1.

To evaluate the performance of all reviewed indices, see Table 1, the studied images were manually segmented by an expert. The obtained images were considered as a ground truth.

An example of the segmentation process is depicted in Figure 3. First, we selected the water indices with an accuracy value greater than a threshold of 0.97. This parameter was tuned manually. If we select a too high value, the number of WI is too small, if we select a very low value the number of WI could be very high and the quality of some WI could be low. Therefore, there is trade-off. In practice, we would like to dispose a good number of WI (more than 3 because of the fusion step, see Figure 1) with high accuracy. We found experimentally that 0.97 met these requirements. Afterwards, these indices are clustered in three groups, see Fig. 3(a), and for each group we maximize the Fisher's criterion which gives the weights of the linear combination (1) obtaining the image in Fig. 3(b) from which we compute the likelihoods for each class, see Figures 3(a) y 3(d). Finally, the segmentation is depicted in Fig. 4.

A. COMPARISON MEASURES

For validation purposes we use several comparison measures which are based on the confusion matrix for binary class classification problems [35], [36]. These measures allow us to assess the performance of algorithms. The performance measure we used for comparing the algorithms are: overall accuracy, recall, precision and Cohen's kappa [37], i.e.,

$$\text{Overall accuracy} = \frac{TP + TN}{TP + FP + FN + TN}, \tag{7}$$

$$\text{Recall} = \frac{TP}{TP + FN}, \tag{8}$$

$$\text{Precision} = \frac{TP}{TP + FP}, \tag{9}$$

where TP is the true positive, TN is the true negative, FP is the false positive and FN is the false negative.

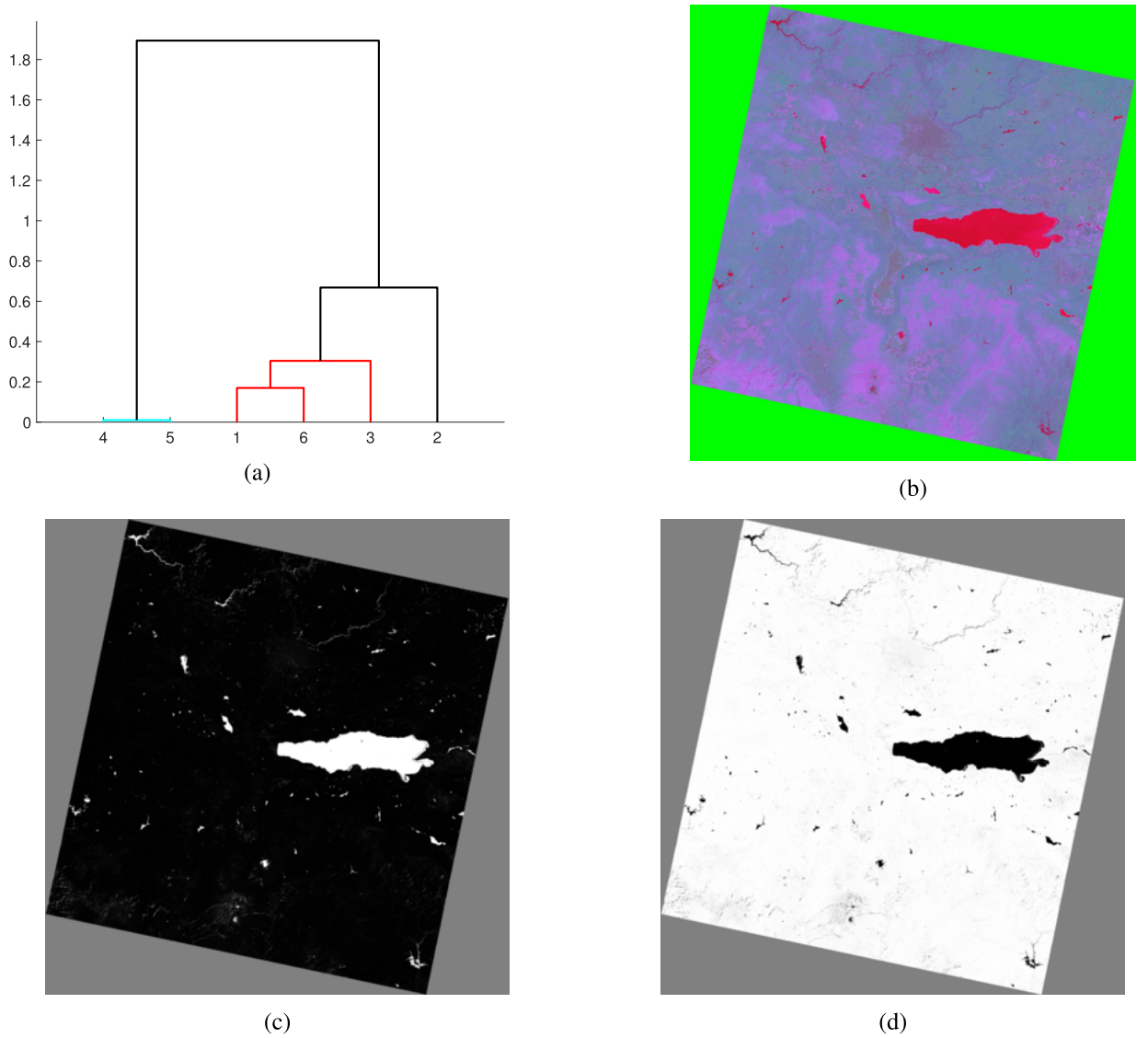

FIGURE 3. (a) Hierarchical clustering of water indices 1-NDWI, 2-MNDWI, 3-NDVI, 4-AWEInsh, 5-AWEIsh and 6-NDWI5. Dendrogram for clustering water indices applied to a sample taken from Chapala lake. (b) New image created with (1) and the following weights for the linear combination $\alpha_1 = [0.0237, 0.9997]$, $\alpha_2 = [-0.1674, -0.5467, -0.8204]$ and $\alpha_3 = [1]$ with corresponding water indices [AWEInsh, AWEIsh], [NDWI, NDVI, NDWI5] and [MNDWI] respectively. Weights were calculated through a maximization of the Fisher's criterion. Inputs of the GMMF Algorithm, (c) likelihood to belong to water body, (d) likelihood to belong to non-water.

The overall accuracy (7) is the number of correct classifications divided by the total number of classified data. The recall (8), in our case, corresponds to the proportion of pixels in the water body that are successfully classified, i.e., it is the ratio between true positives and the total number of positives (true positives and false negatives). The recall is also called *true positive rate* or *sensitivity*. The Precision (9) is a measure of the accuracy of the water class and it is the ratio between the number of correctly predicted data of the water class divided by the total number of classified data in the water class. Cohen's kappa [37] measures the agreement between two raters, in which each one classifies N items into K mutually exclusive categories.

VI. EXPERIMENTAL RESULTS AND DISCUSSION

In the case of the proposal, we consider three alternatives, see Section III, to combine the water indices: linear discriminant analysis (lda), the selection of the best index for each cluster (best), and the average of water indices for each cluster (average). Similarly, we compare two variants for SVM: the linear and Radial Basis Function (rbf) alternatives. The experiments are carried out to the three water bodies considered, some discussion is given for each of them, and a general analysis is also provided at the end of this section. The results are shown in Tables 3, 4 and 5. In bold we show the method with best results and in italic and bold the methods with the second best results.

TABLE 3. Chapala lake. numerical comparison. In bold the method with best results and in italics and bold the methods with the second best results.

Chapala lake	MNDWI	WRI	NDVI	SVM		Proposal		
				linear	rbf	lda	best	average
Accuracy	0.9943	0.9959	0.9955	0.9944	0.9940	**0.9972**	***0.9971***	***0.9971***
Kappa	0.9144	0.9319	0.9289	0.9159	0.9109	**0.9557**	***0.9544***	0.9549
Recall	0.9777	0.9052	0.9541	0.9798	**0.9853**	0.9799	***0.9809***	0.9797
Presicion	0.8640	0.9648	0.9094	0.8648	0.8522	**0.9354**	0.9321	***0.9341***

TABLE 4. Infiernillo reservoir. numerical comparison.

Infiernillo reservoir	MNDWI	WRI	NDVI	SVM		Proposal		
				linear	rbf	lda	best	average
Accuracy	0.9927	0.9972	0.9955	0.9958	0.9970	0.9975	***0.9978***	**0.9979**
Kappa	0.9358	0.9744	0.9600	0.9632	0.9735	0.9777	***0.9809***	**0.9813**
Recall	0.9830	0.9696	***0.9911***	**0.9913**	0.9907	0.9843	0.9909	***0.9911***
Precision	0.8999	**0.9823**	0.9353	0.9409	0.9599	0.9737	0.9733	***0.9739***

TABLE 5. Nezahualcoyotl reservoir. numerical comparison.

Nezahualcoyotl reservoir	MNDWI	WRI	NDVI	SVM		Proposal		
				linear	rbf	lda	best	average
Accuracy	0.9858	0.9927	0.7694	0.9852	0.9850	0.9918	**0.9942**	***0.9940***
Kappa	0.7144	0.8295	0.1066	0.6979	0.6962	0.8129	**0.8596**	***0.8560***
Recall	***0.9993***	0.9950	**0.9999**	0.9769	0.9776	0.9917	0.9941	0.9939
Precision	0.5641	0.7166	0.0736	0.5514	0.5492	**1.0000**	**1.0000**	**1.0000**

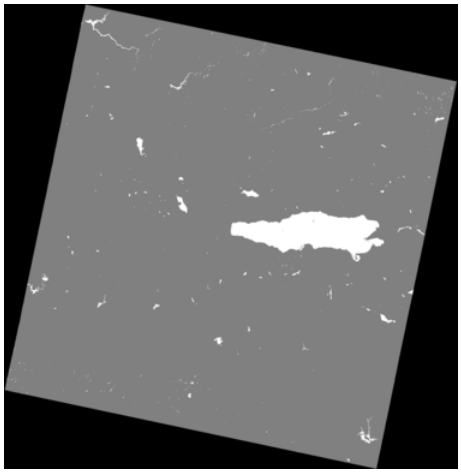

FIGURE 4. Segmentation result of Chapala lake using GMMF with likelihoods, Fig. 3(c), computed from Fig. 3(b). Regions in white correspond to water bodies and in gray to non-water bodies. Regions of non-interest are areas in black.

A. CHAPALA LAKE

Obtained results for Chapala lake are shown in Table 3. As it can be seen, the results are very good for almost all the used indices. Nevertheless, it can be appreciated indeed that the proposed new approach outperforms the previous methods in accuracy, Kappa index and precision. With respect to recall, the SVM rbf obtains the best result, but it is important to notice that our method is ranked in second place. On the other hand, the overall accuracy is better for the proposed approach, which means that the proportion of well-classified pixels are better managed by the proposal.

B. INFIERNILLO RESERVOIR

Table 4 presents the results obtained for the Infiernillo water body; as it can be seen, the obtained results are very good for almost all the used indices. The proposed approach, using the average of water indices per cluster, obtains the best accuracy 0.9979 and Kappa 0.9813 results; obtained values for recall and precision are ranked in second position, with very low difference with the best ones SVM linear and WRI respectively.

C. NEZAHUALCOYOTL RESERVOIR

Obtained results for the Nezahualcoyotl reservoir can be seen in Table 5. As it can be seen, Kappa indices are in general not good for the state of the art methods, which obtain values in the range 0.1066 to 0.8295, value which is improved up to 0.8596 by the new proposed approach. The proposed approach also obtains the best accuracy among all of the used methods 0.9942 and 0.9940, slightly better than the third one 0.9927 obtained by WRI. As a matter of fact, the obtained precision is 1.0000 (actually the number of false positives in our proposals is very small compared to the true positives and the precision is practically 1), and that value combined with the good recall gives this accuracy result.

The new proposed approach obtained a 100% precision value, which is significantly better than the second best value (71.66%) obtained using the WRI index; the proposed approach is the one which obtains the best accuracy as well (99.42%). This indicates the appropriateness of the proposed approach for water detection in different places, morphologies and sizes.

The reviewed methods are competitive in their overall accuracy, however the proposed method not only presents the best overall accuracy, but is also more consistent with respect to the remaining comparison measures. The new method outperforms, in general, the kappa index and precision value for all the considered water bodies, see for example Table 5. Notwithstanding, our method requires more computational time due to the probabilistic segmentation (PS) step. The PS can easily be implemented in parallel with CUDA using a NVIDIA GPU and one can obtain binary segmentation in real time, see [38] for details.

VII. CONCLUSIONS

In this paper a new approach has been presented to deal with water bodies detection in satellite images; the main idea is to select and combine existing water indices which best fits with the characteristics of the studied water body. To this end, we select the water indices with best performance according to its accuracy, then the selected indices are clustered, and finally, the indices in each cluster are combined and used to perform a *water-non water* classification process.

Obtained results are very good, outperforming state-of-the-art approaches in almost all of the comparison measures considered in our study. Especially in accuracy and Kappa, the results are the best ones for all the considered water bodies.

It is worth mentioning that the new proposed approach is able to adapt to the characteristics of the water body in study, which helps to improve water indices accuracy. In fact, the method combines the best water indices found for a given water body, being dynamically adapted to the environment. It can be inferred as well that the formula used to classify water-non water pixels can vary for the same place in different periods of time, or in different weather conditions, which made it more feasible to deal with temporal evolution of the water presence.

As Future Works some lines remain open:

More combinations of water indices can be tested; as a matter of fact, the list of used indices can be updated and newer indices can be included in the combinations as they appear in the literature.

Other line which could improve the water detection capability is the use of Multi-classifiers instead of the one used in this paper. This is another research more related with Machine Learning, more precisely with the searching for the most adequate classifier to deal with a given classification task.

Another line that the authors of this paper have in mind is to use more image collections, and of different sensors, in order to extend the paradigm.

REFERENCES

[1] S. D. Jawak, K. Kulkarni, and A. J. Luis, "A review on extraction of lakes from remotely sensed optical satellite data with a special focus on cryospheric lakes," *Adv. Remote Sens.*, vol. 4, pp. 196–213, 2015.

[2] J. MacQueen, "Some methods for classification and analysis of multivariate observations," in *Proc. 5th Berkeley Symp. Math. Statist. Probab.*, vol. 1. 1967, pp. 281–297.

[3] T. Z. Phyo, A. S. Khaing, and H. M. Tun, "Classification of cluster area for satellite image," *Int. J. Sci. Technol. Res.*, vol. 4, no. 6, pp. 393–397, 2015.

[4] G. H. Ball and D. J. Hall, "ISODATA, a novel method of data analysis and pattern recognition," Stanford Res. Inst., Menlo Park, CA, USA, Tech. Rep., 1965. [Online]. Available: http://www.dtic.mil/dtic/tr/fulltext/u2/699616.pdf

[5] B. C. Ko, H. H. Kim, and J. Nam, "Classification of potential water bodies using Landsat 8 oli and a combination of two boosted random forest classifiers," *Sensors*, vol. 15, no. 6, pp. 13763–13777, 2015.

[6] T. D. Acharya, D. H. Lee, I. T. Yang, and J. K. Lee, "Identification of water bodies in a Landsat 8 oli image using a J48 decision tree," *Sensors*, vol. 16, no. 7, p. 1075, 2016.

[7] C. Cortes and V. Vapnik, "Support-vector networks," *Mach. Learn.*, vol. 20, no. 3, pp. 273–297, 1995.

[8] F. Rosenblatt, "The perceptron: A probabilistic model for information storage and organization in the brain," *Psychol. Rev.*, vol. 65, no. 6, pp. 386–408, 1958.

[9] S. K. Mcfeeter, "The use of the normalized difference water index (NDWI) in the delineation of open water features," *Int. J. Remote Sens.*, vol. 17, no. 7, pp. 1425–1432, 1996.

[10] Y. O. Ouma and R. Tateishi, "A water index for rapid mapping of shoreline changes of five East African Rift Valley lakes: An empirical analysis using Landsat TM and ETM+ data," *Int. J. Remote Sens.*, vol. 27, no. 15, pp. 3153–3181, 2006.

[11] H. Xu, "Modification of normalised difference water index (NDWI) to enhance open water features in remotely sensed imagery," *Int. J. Remote Sens.*, vol. 27, no. 14, pp. 3025–3033, 2006.

[12] L. Shen and C. Li, "Water body extraction from Landsat ETM+ imagery using Adaboost algorithm," in *Proc. 18th Int. Conf. Geoinformatics*, Jun. 2010, pp. 1–4.

[13] K. Rokni, A. Ahmad, A. Selamat, and S. Hazini, "Water feature extraction and change detection using multitemporal Landsat imagery," *Remote Sens.*, vol. 6, no. 5, pp. 4173–4189, 2014.

[14] G. L. Feyisa, H. Meilby, R. Fensholt, and S. R. Proud, "Automated Water Extraction Index: A new technique for surface water mapping using Landsat imagery," *Remote Sens. Environ.*, vol. 140, pp. 23–35, Jan. 2014.

[15] S. Jin and S. A. Sader, "Comparison of time series tasseled cap wetness and the normalized difference moisture index in detecting forest disturbances," *Remote Sens. Environ.*, vol. 94, no. 6, pp. 364–372, 2005.

[16] J. W. Rouse, "Monitoring the vernal advancements and retrogradation of natural vegetation," NASA/GSFC, Greenbelt, MD, USA, Tech. Rep., 1974. [Online]. Available: https://ntrs.nasa.gov/archive/nasa/casi.ntrs.nasa.gov/19740004927.pdf

[17] M. A. Hardisky, V. Klemas, and R. M. Smart, "The influence of soil salinity, growth form, and leaf moisture on the spectral radiance of Spartina alterniflora canopies," *Photogramm. Eng. Remote Sens.*, vol. 49, no. 1, pp. 77–83, 2005.

[18] K. Mishra and P. R. C. Prasad, "Automatic extraction of water bodies from Landsat imagery using perceptron model," *J. Comput. Environ. Sci.*, vol. 2015, Dec. 2015, Art. no. 903465. [Online]. Available: http://downloads.hindawi.com/journals/jces/2015/903465.pdf, doi: 10.1155/2015/903465.

[19] G. Sarp and M. Ozcelik, "Water body extraction and change detection using time series: A case study of Lake Burdur, Turkey," *J. Taibah Univ. Sci.*, vol. 11, no. 3, pp. 381–391, 2017.

[20] G. Kaplan and U. Avdan, "Object-based water body extraction model using Sentinel-2 satellite imagery," *Eur. J. Remote Sens.*, vol. 50, no. 1, pp. 137–143, 2017.

[21] G. Câmara, R. C. M. Souza, U. M. Freitas, and J. Garrido, "SPRING: Integrating remote sensing and GIS by object-oriented data modelling," *Comput. Graph.*, vol. 20, no. 3, pp. 395–403, 1996.

[22] Y. He, X. Zhang, and L. Hua, "Object-based distinction between building shadow and water in high-resolution imagery using fuzzy-rule classification and artificial bee colony optimization," *J. Sensors*, vol. 2016, Jun. 2016, Art. no. 2385039. [Online]. Available: https://www.tandfonline.com/doi/pdf/10.1080/22797254.2017.1297540?needAccess=true

[23] F. E. Oliva, O. S. Dalmau, and T. E. Alarcón, "Classification of different vegetation types combining two information sources through a probabilistic segmentation approach," in *Human-Inspired Computing and Its Applications* (Lecture Notes in Artificial Intelligence), vol. 8856. Springer, Nov. 2015, pp. 327–335. [Online]. Available: https://link.springer.com/chapter/10.1007/978-3-319-27101-9_29

[24] O. S. Dalmau, T. E. Alarcón, and F. E. Oliva, "Crop classification in satellite images through probabilistic segmentation based on multiple sources," *Sensors*, vol. 17, no. 6, p. 1373, 2017.
[25] J. Lacaux, Y. M. Tourre, C. Vignolles, J. A. Ndione, and M. Lafaye, "Classification of ponds from high-spatial resolution remote sensing: Application to Rift Valley fever epidemics in Senegal," *Remote Sens. Environ.*, vol. 106, no. 1, pp. 66–74, 1998.
[26] D. K. Hall, J. L. Foster, D. L. Verbyla, A. G. Klein, and C. S. Benson, "Assessment of snow-cover mapping accuracy in a variety of vegetation-cover densities in Central Alaska," *Remote Sens. Environ.*, vol. 66, no. 2, pp. 129–137, 1998.
[27] D. Chen, J. Huang, and T. J. Jackson, "Vegetation water content estimation for corn and soybeans using spectral indices derived from MODIS near- and short-wave infrared bands," *Remote Sens. Environ.*, vol. 98, nos. 2–3, pp. 225–236, 1998.
[28] N. Otsu, "A threshold selection method from gray-level histograms," *IEEE Trans. Syst., Man, Cybern.*, vol. SMC-9, no. 1, pp. 62–66, Jan. 1979.
[29] S. C. Johnson, "Hierarchical clustering schemes," *Psychometrika*, vol. 32, no. 3, pp. 241–254, 1967.
[30] S. Theodoridis and K. Koutroumbas, *Pattern Recognition*, 4th ed. Amsterdam, The Netherlands: Elsevier, 2009.
[31] J. Lira, "Segmentation and morphology of open water bodies from multispectral images," *Int. J. Remote Sens.*, vol. 27, no. 18, pp. 4015–4038, 2006.
[32] U.S. Geological Survey. (2016). *Landsat 8 (L8) Data Users Handbook*. [Online]. Available: http://landsat.usgs.gov/landsat-8-l8-data-users-handbook
[33] Y. Yang *et al.*, "Landsat 8 OLI image based terrestrial water extraction from heterogeneous backgrounds using a reflectance homogenization approach," *Remote Sens. Environ.*, vol. 171, pp. 14–32, Dec. 2015.
[34] G. Chander, B. L. Markham, and D. L. Helder, "Summary of current radiometric calibration coefficients for Landsat MSS, TM, ETM+, and EO-1 ALI sensors," *Remote Sens. Environ.*, vol. 113, no. 5, pp. 893–903, 2009.
[35] F. Provost and R. Kohavi, "On applied research in machine learning," *Mach. Learn.*, vol. 30, nos. 2–3, pp. 127–132, 1998.
[36] M. Sokolova and G. Lapalme, "A systematic analysis of performance measures for classification tasks," *Inf. Process. Manag.*, vol. 45, no. 4, pp. 427–437, 2009.
[37] J. Cohen, "A coefficient of agreement for nominal scales," *Edu. Psychol. Meas.*, vol. 20, no. 1, pp. 37–46, 1960.
[38] F. J. Hernandez-Lopez and M. Rivera, "Binary segmentation of video sequences in real time," in *Proc. 9th Mexican Int. Conf. Artif. Intell.*, Nov. 2010, pp. 163–168.

GABRIELA CALVARIO SÁNCHEZ received the bachelor's degree in computer science engineering from the University of Guadalajara in 2003 and the master's degree in space science and technology in the field of satellite image processing from the Faculty of Engineering, Bilbao, Spain, in 2013. She is currently pursuing the Ph.D. degree with the Faculty of Informatics, University of the Basque Country. Her research interests are focused in the field of satellite and aerial image processing, machine learning paradigms, remote sensing, GIS, and computer vision.

OSCAR DALMAU received the B.Sc.Ed. degree in mathematics from ISP Manzanillo Cuba in 1989, and the M.Sc. degree in computer science and industrial mathematics and the Ph.D. degree in computer science from the Center of Research in Mathematics (CIMAT), Guanajuato, Mexico, in 2004 and 2010, respectively. He is currently with CIMAT. His research interests lie in the areas of machine learning, optimization, image processing, and computer vision.

TERESA E. ALARCÓN received the Title of Engineer degree in automated systems of management from the Moscow Institute of Direction "Sergo Orchonikidze," Russia, in 1989, the master's degree in digital image processing from the "José Antonio Echeverría" Polytechnic Institute, Cuba, in 1999, and the Ph.D. degree in computer science from the Center for Mathematics Research, Guanajuato, Mexico, in 2007. She is currently an Associate Professor with the Computational Sciences and Engineering Department, University of Guadalajara, Valley Campus, Ameca. Her field of research is digital image processing, including filtering, segmentation, and pattern recognition topics.

BASILIO SIERRA is currently a Full-Time Professor with the Computer Sciences and Artificial Department, University of the Basque Country. He is focused on supervised classification, one-class classification, machine learning, pattern recognition, and computer vision. He leads the University Robotics Team. He has published more than 40 journal papers, several international conference papers, and book chapters. His research interests are focused on improving robot autonomy by means of machine learning paradigms.

CARMEN HERNÁNDEZ is currently a Full-Time Professor with the Computer Sciences and Artificial Department, University of the Basque Country, and a PhD Collaborator with the Centro de Investigação e Tecnologias Agro-ambientais e Biológicas, Universidade de Trás-os-Montes e Alto Douro, Vila Real, Portugal. She is focused on GIS, spatial statistics, satellite image processing, machine learning, pattern recognition, and combinatorial optimization. Her research interests are focused on remote sensing and image processing.